



## Facilitating intermetallic formation in wire bonding by applying a pre-ultrasonic energy

H. Xu <sup>a,\*</sup>, V.L. Acoff <sup>a</sup>, C. Liu <sup>b</sup>, V.V. Silberschmidt <sup>b</sup>, Z. Chen <sup>c</sup>

<sup>a</sup> Department of Metallurgical and Materials Engineering, The University of Alabama, Tuscaloosa, AL 35487, United States

<sup>b</sup> Wolfson School of Mechanical and Manufacturing Engineering, Loughborough University, Loughborough LE11 3TU, United Kingdom

<sup>c</sup> School of Materials Science and Engineering, Nanyang Technological University, Nanyang Avenue, Singapore 639798, Singapore

### ARTICLE INFO

#### Article history:

Received 30 March 2011

Accepted 21 June 2011

Available online 30 June 2011

#### Keywords:

Wire bonding

Intermetallic compounds

Interface

Ultrasonic energy

Bonding mechanism

### ABSTRACT

It is conventionally believed that wire bonding initiates at the periphery of the contact area and no bonding occurs in the central area. However, this paper demonstrated that two bonding patterns exist, and are determined by bonding processes. If a selected pre-ultrasonic energy is applied, intermetallic compounds initiate in both peripheral and central area of bonds. However, if a pre-ultrasonic energy is absent, intermetallic compounds are only present at the peripheral area as conventionally reported. The application of the pre-ultrasonic energy significantly improves bonding strength, from 66.8 to 94.5 MPa for 20  $\mu\text{m}$  Au wire bonds, due to the intermetallic compounds of greater structured integrity. Two different mechanisms are respectively proposed to account for the intermetallic formation in the center and periphery of the bond interface.

© 2011 Elsevier B.V. All rights reserved.

### 1. Introduction

Wire bonding is a versatile interconnection technique in micro-electronic packaging industry due to its nature of the process including low cost, self-cleaning capability, high yield rate, flexibility and reliability. Over 90% interconnections of integrated circuits (ICs) and other semiconductor chips are wire bonded [1]. A variety of investigations have been carried out to reveal bonding mechanism and effects of processes on bondability and reliability [2–6]. It is conventionally believed that wire bonding initiates near the periphery and no bonding occurs in the central areas of the bonds [7–13]. Harman et al. [7,8] applied a low ultrasonic power and bonding force, so the wire does not stick on the pads, but leaves footprints on the pads. They reported that the wire-to-pad micro-joints initiate near the perimeter and spread towards the center of the contact area with time. With a long bonding duration, the wire could not be lifted up without tearing the pad. In such a case, mechanical removal of the wire is obliged to view the footprints on the pads. Lum et al. [9] employed this method to investigate the effect of ultrasonic energy on the bond formation in ultrasonic Al wedge bonding on Cu pads, and reported that bonding initiates at the periphery and develops inwards with an increase in ultrasonic power. Zhou et al. [10] and Lum et al. [11] studied the footprints of thermosonic gold ball bonding on Al pads and Cu pads, respectively. Similar to ultrasonic wedge bonding, the ball-to-pad

microjoints tend to be initially formed around the perimeter. Qi et al. [14] observed the distribution of intermetallic compounds (IMCs) on the gold ball bottom by etching the Al pads away and proposed that bonding only occurs at the periphery of the bonds. However, this paper found that bonding takes place in the central area of bond interface as well as the periphery by adding a pre-ultrasonic energy on the course of the initial ball-to-pad contact, and the bonding strength accordingly increases significantly.

### 2. Materials and methods

Thermosonic gold/copper wire bonding was conducted with an ASM Eagle 60AP ball/wedge automatic bonder. Both copper and gold wires are 99.99 wt.% and 20  $\mu\text{m}$  in diameter. The aluminium pad is 1  $\mu\text{m}$  thick on  $\text{SiO}_2/\text{Si}$ . An electrical flame off (EFO) process produced a free air ball (FAB) at the bonding wire tip. After cooling, the gold or copper ball was transferred onto the Al pad to form the bond using a combination of a normal force, transverse ultrasonic vibration and heat (Table 1). A three-stage-bonding process is developed: (i) standby stage, (ii) contact stage and (iii) bonding stage. A standby stage is the initial stage when a ball is touched on the bond pad (the ultrasonic energy added at this stage is termed as pre-ultrasonic energy), followed by a contact stage and a bonding stage. Parameter levels 1 and 2 are used for gold wire bonding, with the former without a pre-ultrasonic power and the latter possessing a pre-ultrasonic power. Parameter level 3 is employed for copper wire bonding with a pre-ultrasonic power. Because ultrasonic power developed in the piezoceramic stack

\* Corresponding author. Tel.: +1 205 348 4473.

E-mail addresses: [HXu14@bama.ua.edu](mailto:HXu14@bama.ua.edu), [huixu.hit@gmail.com](mailto:huixu.hit@gmail.com) (H. Xu).

**Table 1**  
Wire bonding parameters.<sup>a</sup>

Bonding parameters	Au (level 1)	Au (level 2)	Cu (level 3)
Pre-ultrasonic power (DAC) <sup>b</sup>	0	10 (175.0 nm)	12 (210.0 nm)
Contact power (DAC)	5 (87.5 nm)	5 (87.5 nm)	10 (175.0 nm)
Contact force (mN)	100	100	220
Contact duration (s)	0.002	0.002	0.003
Bonding power (DAC)	35 (612.5 nm)	35 (612.5 nm)	36 (630.0 nm)
Bonding force (mN)	80	80	180
Bonding duration (s)	0.006	0.006	0.006
Substrate temperature (°C)	175	175	175

<sup>a</sup> Ultrasonic amplitudes of the capillary tip are listed in brackets.

<sup>b</sup> DAC is an ASM internal energy unit. It is the abbreviation of digital to analog conversion.

was transferred with loss, the actual ultrasonic amplitudes at the capillary tip were measured by a laser interferometer (Table 1); the ultrasonic frequency was maintained at 138 kHz.

Electron transparent cross-sections of the bonds were prepared with a dual-beam FIB system (FEI Nova 600 NanoLab) and scanning electron microscopy (SEM) was conducted *in situ*. TEM analysis was performed using a JEOL 2100F system at 200 kV. Shear tests were conducted with a DAGE 4000 microtester at a tool height of 3  $\mu\text{m}$  to evaluate the bonding strength. The shear strength was expressed as shear force per unit area.

### 3. Results

#### 3.1. Gold wire bonding

In Au–Al bonds produced without a pre-ultrasonic energy (level 1, Table 1), IMCs are only present at peripheral area of the interface (Fig. 1a and a'), consistent with a series of previous studies [7–12]. However, if a pre-ultrasonic energy is applied (level 2, Table 1), IMCs initiate at both peripheral and central area (Fig. 1b and b'). The shear force and shear strength correspondingly increases from 0.075 to 0.112 N and from 66.8 to 94.5 MPa, respectively (Fig. 2).

#### 3.2. Copper wire bonding

The Cu–Al interface formed with a pre-ultrasonic power (level 3, Table 1) can be generally divided into three zones in terms of the amount of IMCs (Fig. 3). The central areas (Zone-1, Fig. 3a) consist of an almost continuous layer of IMCs (Fig. 3b); the peripheral areas (Zone-2, Fig. 3a) contain discontinuous IMCs particles (Fig. 3c); the areas (Zone-3, Fig. 3a) between the center and periph-

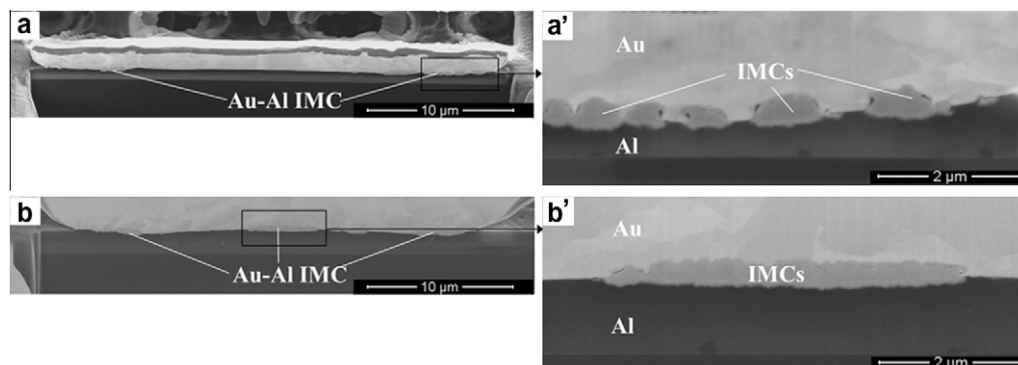


**Fig. 1.** Dependence of IMC distribution on pre-ultrasonic energy: (a and a') IMCs only at the periphery of the bond interface without pre-ultrasonic energy; (b and b') IMCs at both the periphery and center with pre-ultrasonic energy. (See Table 1 for detailed parameters).

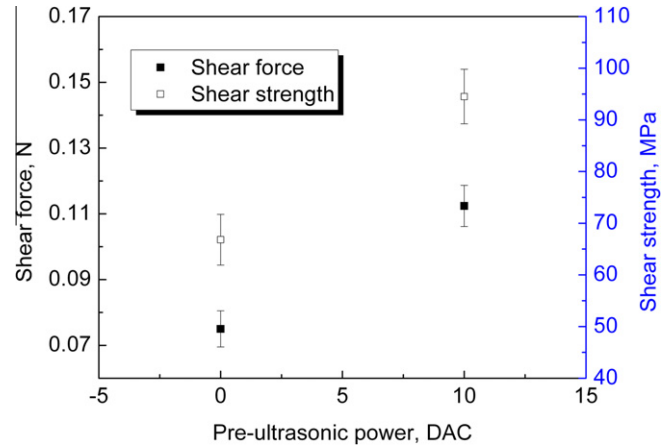


**Fig. 2.** Application of pre-ultrasonic power promotes IMCs of greater structured integrity that increases shear force and shear strength. The error bars are the standard deviation for 20 measured samples.

ery are almost free of IMCs (Fig. 3d). This is similar to IMC distribution at the Au–Al interface produced with a pre-ultrasonic power where IMCs are present at both central and periphery area, though the Cu–Al IMCs (~30 nm) are much thinner than Au–Al IMCs (~300 nm).

### 4. Discussions

The results show that in the bonds produced without a pre-ultrasonic power (as for conventional process), IMCs are only present at the periphery of the bond interface; however, by application of a pre-ultrasonic power, IMCs initiate in both peripheral and central area of bonds, which significantly improves bonding strength (e.g. from 66.8 to 94.5 MPa for Au–Al bonds).

It is known that a ubiquitous native alumina overlayer is on the aluminum pad and the nucleation of IMCs is associated with the fragmentation of such oxide layer, since it acts as a barrier to diffusion. Xu et al. [2,3] by high resolution transmission electron microscopy (HRTEM) reported that the ultrasonic vibration under certain pressure and heat partially fragments the native alumina layer, providing the pathways for metal interdiffusion. This promotes IMC formation ( $\text{CuAl}_2$  in Cu–Al bonds,  $\text{Au}_4\text{Al}$  and  $\text{AuAl}_2$  in Au–Al bonds) and consequently improves the bonding strength. IMCs are absent in some areas where oxide layer remains. In this study, we found that IMCs exist in both peripheral and central interface, suggesting that the alumina layer was disrupted in both areas. The formation of IMCs at the periphery is usually explained by “microslip” theory. In such model for a compliance of two

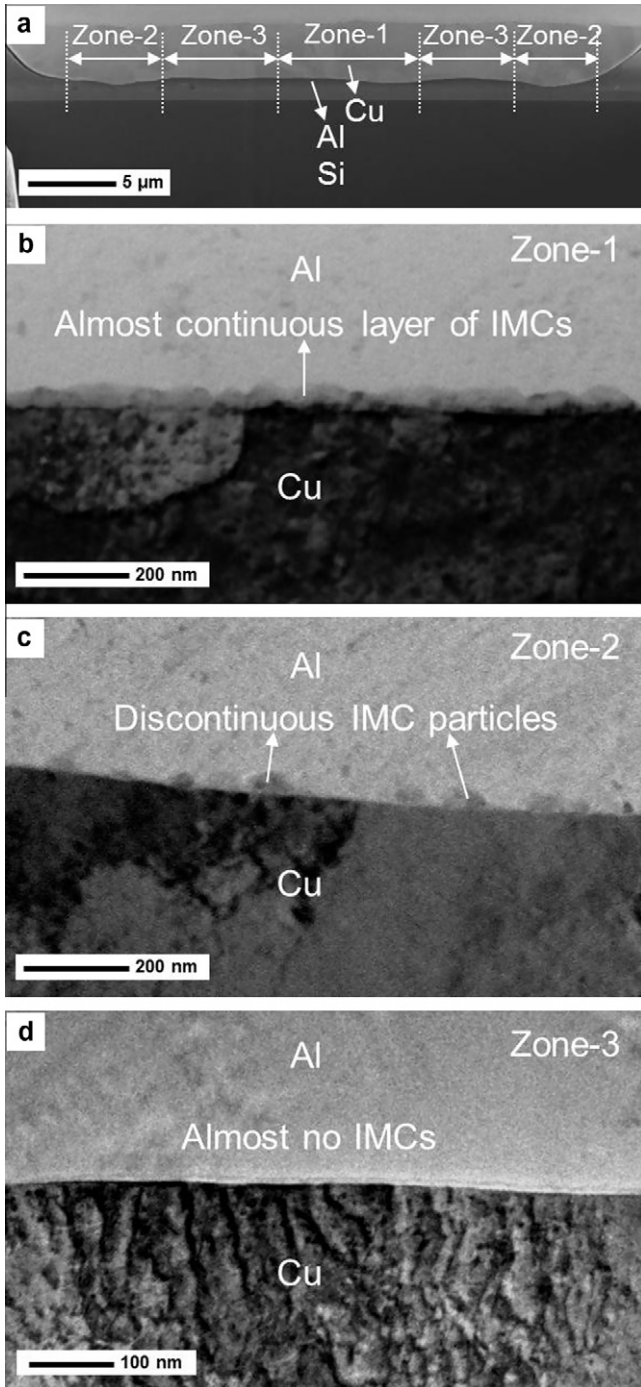


**Fig. 3.** Distribution of IMCs at Cu–Al interface: (a) general view of Cu–Al interface; (b) details of Zone-1 in (a) showing almost continuous layer of IMCs in the central interface; (c) details of Zone-2 in (a) showing discontinuous IMCs particles in the peripheral interface; (d) details of Zone-3 in (a) showing almost no IMCs in the area between center and periphery.

perfectly elastic spheres subjected to both a normal force  $P_n$  and a tangential force  $P_t$  [15,16],

$$P_n(x) = \frac{P_n}{2\pi a^3} (a^2 - x^2)^{1/2}, \quad (1)$$

$$P_t(x) = \frac{P_t}{2\pi a} (a^2 - x^2)^{1/2}, \quad (2)$$

where  $P_t(x)$  and  $P_t$  are the distribution of  $P_n$  and  $P_t$  (that in wire bonding are determined by bonding force and ultrasonic energy, respectively) over the contact area respectively,  $x$  the radial coordinate from the center of the contact area and  $a$  the radius of this area. The magnitude of normal traction reduces from the center of the contact surface to the edge, and that of the tangential traction rises from one half of the average at the center to infinity at the edge, therefore, there will be slip at the periphery and possibly stationary in the center. The slip at the periphery causes the fracture of the oxide, facilitating the IMC formation.

The “microslip” model deals with the normal and tangential traction when two spheres are in contact and deformed. However, the ball deformation process during bonding is a dynamic process, including standby stage, contact stage and bonding stage, and the “microslip” model only explains the nature for the stages when balls have been already mashed. During the initial contact of the ball on the Al pad, the application of pre-ultrasonic power can disrupt the oxide at the contact area – the central region of the bond interface, consistent with the “fretting” theory [17]. However, if the pre-ultrasonic power is not applied, no fretting occurs during the initial stage of bonding, therefore, no IMCs form in the central interface of the bonds, as conventionally observed. It is also noted that a continuous layer of IMC may be produced if a high-level ultrasonic power is applied during the whole bonding process.

### 5. Conclusion

The nucleation sites of IMCs during wire bonding are controlled by bonding process. IMCs initiate at the periphery of the bond interface and are absent in the center as conventional process proceeds without a pre-ultrasonic energy. However, application of a pre-ultrasonic energy facilitates IMC formation in the central area of the bond interface, which correspondingly increases the bonding strength.

### References

- [1] G.G. Harman, Wire Bonding in Microelectronics, third ed., McGraw-Hill, New York, London, 2010.
- [2] H. Xu, C. Liu, V.V. Silberschmidt, S.S. Pramana, T.J. White, Z. Chen, M. Sivakumar, V.L. Acoff, Journal of Applied Physics 108 (2010) 113517.
- [3] H. Xu, C. Liu, V.V. Silberschmidt, S.S. Pramana, T.J. White, Z. Chen, Scripta Materialia 61 (2009) 165.
- [4] J. Li, L. Han, J. Duan, J. Zhong, Applied Physics Letters 90 (2007) 242902.
- [5] I. Lum, H. Huang, B.H. Chang, M. Mayer, D. Du, Y. Zhou, Journal of Applied Physics 105 (2009) 024905.
- [6] S. Murali, N. Srikanth, C.J. Vath Iii, Materials Letters 58 (2004) 3096.
- [7] G.G. Harman and K.O. Leedy, In 10th Annual Reliability Physics, Las Vegas, USA (1972) 49.
- [8] G.G. Harman, J. Albers, IEEE Transactions on Parts, Hybrids, and Packaging 13 (1977) 406.
- [9] I. Lum, M. Mayer, Y. Zhou, Journal of Electronic Materials 35 (2006) 433.
- [10] Y. Zhou, X. Li, N.J. Noolu, IEEE Transactions on Components and Packaging Technologies 28 (2005) 810.
- [11] I. Lum, J.P. Jung, Y. Zhou, Metallurgical and Materials Transactions A 36 (2005) 1279.
- [12] H.J. Ji, M.Y. Li, C.Q. Wang, J.W. Guan, H.S. Bang, Journal of Materials Processing Technology 182 (2006) 202.
- [13] H. Xu, C. Liu, V.V. Silberschmidt, Z. Chen, J. Wei, Journal of Materials Processing Technology 210 (2010) 1035.
- [14] J. Qi, N.C. Hung, M. Li, D. Liu, Scripta Materialia 54 (2006) 293.
- [15] R.D. Mindlin, Journal of Applied Mechanics 71 (1949) 259.
- [16] S. Timoshenko, J.N. Goodier, Theory of Elasticity, McGraw-Hill, New York, 1951.
- [17] A.P. Hulst, C. Lasance, Welding Journal 57 (1978) 19.